Geochemistry Geophysics Geosystems G3

Published by AGU and the Geochemical Society

Article
Volume 12, Number 9
13 September 2011
Q09006, doi:10.1029/2011GC003649
ISSN: 1525-2027

Three-dimensional Moho topography in Italy: New constraints from receiver functions and controlled source seismology

R. Di Stefano, I. Bianchi, and M. G. Ciaccio
Istituto Nazionale di Geofisica e Vulcanologia, Via di Vigna Murata 605, Rome I-00143, Italy (raffaele.distefano@ingv.it)

G. Carrara
Instituto Dom Luiz, Faculdade de Ciências da Universidade de Lisboa, Lisbon P-1749-016, Portugal

E. Kissling
Institute of Geophysics, ETH Zurich, Zurich CH-8093, Switzerland

[1] In complex tectonics regions, seismological, geophysical, and geodynamic modeling require accurate definition of the Moho geometry. Various active and passive seismic experiments performed in the central Mediterranean region revealed local information on the Moho depth, in some cases used to produce interpolated maps. In this paper, we present a new and original map of the 3-D Moho geometry obtained by integrating selected high-quality controlled source seismic and teleseismic receiver function data. The very small cell size makes the retrieved model suitable for detailed regional studies, crustal corrections in teleseismic tomography, advanced 3-D ray tracing in regional earthquake location, and local earthquake tomography. Our results show the geometry of three different Moho interfaces: the European, Adriatic-Ionian, and Tyrrhenian. The three distinct Moho are fashioned following the Alpine and Apennines subduction, collision, and back-arc spreading and show medium- to high-frequency topographic undulations reflecting the complexity of the geodynamic evolution.

Components: 9100 words, 7 figures, 1 table.

Keywords: Italy; controlled source seismology; crust; receiver function.

Index Terms: 7218 Seismology: Lithosphere (1236); 8150 Tectonophysics: Plate boundary: general (3040).

Received 6 April 2011; **Revised** 26 July 2011; **Accepted** 26 July 2011; **Published** 13 September 2011.

Di Stefano, R., I. Bianchi, M. G. Ciaccio, G. Carrara, and E. Kissling (2011), Three-dimensional Moho topography in Italy: New constraints from receiver functions and controlled source seismology, *Geochem. Geophys. Geosyst.*, *12*, Q09006, doi:10.1029/2011GC003649.

1. Introduction

[2] The central Mediterranean region (Figure 1) is characterized by micro plate tectonics since early Mesozoic times, due to the opening of the Neo-Tethys ocean (280 My to 200 My ago), causing the fragmentation of the African continental margin, and the opening of the Atlantic ocean (180 My ago to present) with the consequent convergence between the European and Africa-Adria plates [*Stampfli and Borel*, 2002]. Such convergence induced lithosphere subduction, continental collision, and back-arc spreading, featuring high lateral variability in composition and

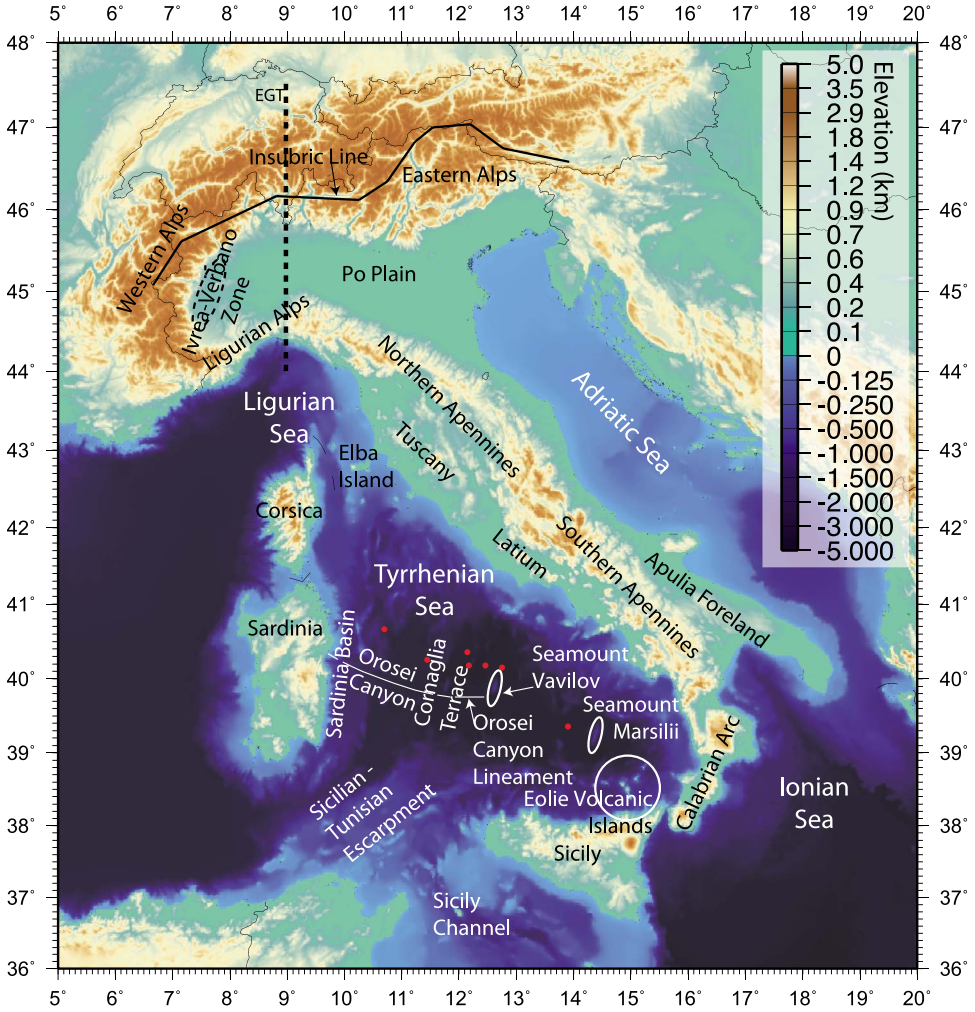

Figure 1. Schematic map of the central Mediterranean region, centered on the Italian peninsula. Blue tones represent negative topographic elevations above sea level; red dots are the locations of the holes of the ODP Leg 107 drilling project [*Kastens et al.*, 1987].

thickness of the lithosphere [*Malinverno and Ryan*, 1986; *Faccenna et al.*, 1996; *Catalano et al.*, 2001; *Doglioni and Carminati*, 2002; *Capitanio and Goes*, 2006; *Di Stefano et al.*, 2009]. As a result of such complexity, half of the 14 crustal types defined by *Mooney et al.* [1998] at global scale are present in the target area [*van der Meijde et al.*, 2003]. Defined as the boundary between the chemically different crust and uppermost mantle, the Moho represents a first-order velocity discontinuity second in magnitude only to the core-mantle boundary. With an equally high-density contrast, the Moho topography is strongly correlated with tectonics and geodynamic processes. In the context of plate tectonics, rheology, and lithosphere evolution, the Moho denotes but the seismically best identifiable indicator of an important intralithospheric layer boundary. It separates the chemically highly differentiated and much lighter crustal rocks from the lithosphere mantle. As a consequence, the undulation and the velocity contrast of the Moho strongly influence the measure of most of the geophysical properties of the Earth, like the gravity field and the propagation of seismic rays [*Waldhauser*, 1996; *Waldhauser et al.*, 1998]. Hence a detailed Moho map is a key requisite for geodynamic modeling, for understanding the evolution and state of lithosphere, and to gain high-resolution detailed models of the upper mantle structure [*Lippitsch et al.*, 2003]. Though a Moho has been observed literally everywhere on the Earth it was searched for [*Mooney et al.*, 1998], the petrology of the two layers that it separates varies significantly depending on the kind of lithosphere (oceanic or continental), on its age, and on its specific evolution. Maps of the Moho topography beneath Italy have been published over the years, based on results from different geophysical methods. *Morelli*

et al. [1967] introduced preliminary isobaths for the Moho in Europe. *Geiss* [1987] produced a map of the Moho topography at the Mediterranean scale, through a least square interpolation of a large number of different geophysical observations collected up to 1986 (see references therein). *Nicolich and Dal Piaz* [1991] presented a simplified sketch map of the Moho isobaths for the Italian region, based only on controlled source seismology (CSS) data. *Suhadolc and Panza* [1989] and *Scarascia et al.* [1994] published compilation maps of the Moho isobaths for the European and Italian areas respectively, both based on revised interpretations of CSS profiles. *Du et al.* [1998] produced the EurID 3-D regionalized model of the European crust and mantle velocity structure including a map of the Moho depth obtained by compiling results of several CSS investigations performed in the area. *Pontevivo and Panza* [2002] defined the characteristics of the lithosphere-asthenosphere system in Italy, based on the analysis of Rayleigh wave dispersion. *Piana Agostinetti and Amato* [2009] compiled the map of the Moho depth for the Italian peninsula (from Tuscany to the Calabrian Arc) based on receiver function data at about 200 seismic stations. *Grad et al.* [2009] produced a new map of the Moho depth beneath Europe based on seismic and gravity data. *Lombardi et al.* [2008] defined the isobaths of the Moho for the western central Alps by applying the receiver function method to 61 permanent and temporary stations. *Waldhauser* [1996] and *Waldhauser et al.* [1998] proposed a new method to determine the 3-D topography and lateral continuity of seismic interfaces and a mean P wave 3-D velocity model by using 2-D-derived CSS reflector data. Such method has been successfully applied to produce original and detailed Moho maps for the Alpine region [*Waldhauser et al.*, 1998; *Lippitsch et al.*, 2003], which has been also included in the map of the European Moho compiled by *Dézes and Ziegler* [2001] and in the new reference model for the European crust by *Tesauro et al.* [2008]. In this paper, we apply the method proposed by *Waldhauser* [1996] to compute a new map of the Moho topography for insular and peninsular Italy, extending southward the results by *Waldhauser et al.* [1998] and *Lippitsch et al.* [2003]. We use both high-quality CSS data and extend the method to include high-quality data from receiver function (RF) studies.

2. Method

[3] The method was originally developed to generate a detailed 3-D velocity model of the crust by integrating Moho depths and velocity information retrieved from CSS 2-D profiles by weighting each data point according to its quality. A full explanation of both the compilation procedure and the interpolation technique for Moho surfaces is reported by *Waldhauser* [1996] and *Waldhauser et al.* [1998]. We summarize fundamental information of the basic method and discuss details about its implementation to include receiver function data. Refraction and reflection seismic techniques—the so-called CSS—are particularly well suited to detect and image seismic interfaces with a significant velocity and/or impedance contrast, the prime example of which is the Moho. Over the years, seismic data have been interpreted with various techniques such as 1-D inversion, 2-D ray tracing methods and synthetic seismogram modeling, to estimate the location of seismic interfaces and associated velocities at various depths along a given profile [*Waldhauser*, 1996; *Waldhauser et al.*, 1998]. Although associating quantitative error estimates to any computation of the Moho depth is of great importance to any usage of the Moho horizon in crustal models, such information are usually not included and only seismic cross sections and the related interpretations are presented in publications [*Kissling*, 1993]. However, large uncertainties are present in the seismic models as an effect of different acquisition and interpretation techniques and/or the complexities of the tectonic settings in the area of investigation. Moreover, CSS methods in particular, are basically 2-D techniques generally applied to 3-D structures, hence before properly using the 2-D seismic sections for the 3-D modeling, the reliability of structural information of published models needs to be assessed, weighted and expressed as spatial uncertainty of the reflector element locations [*Kissling et al.*, 1997]. We here adopt for CSS data the same criteria applied by *Waldhauser et al.* [1998]. We estimate the information quality of reflector elements by using a weighting scheme [*Kissling*, 1993; *Baumann*, 1994] with separate weighting criteria for wide-angle and near-vertical reflection surveys. Reflector elements derived from wide-angle profiles are weighted considering the quality and correlation of the observed phases (W_C), profile orientation relative to the 3-D tectonic setting (W_O), and profile type (i.e., whether the profile is reversed or unreversed) (W_T). A total weighting factor (W_{TOT}) is obtained for each segment of the reflector, by multiplying the individual weights. The Moho interface is generated by interpolating weighted depth values, following the criteria of "highest continuity–least roughness" [*Waldhauser*, 1996] with respect to the data and their error boundaries. Lateral continuity

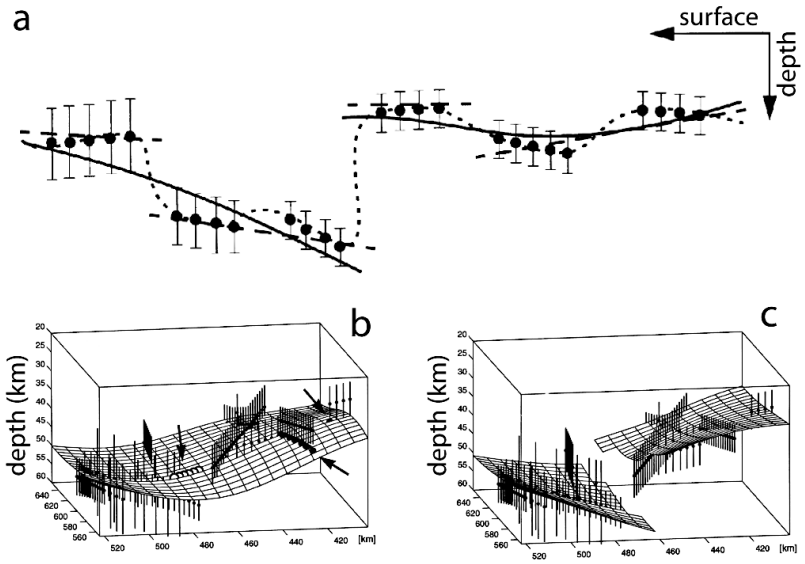

Figure 2. Data and related error boundaries are best fitted by taking into account major offsets of the Moho discontinuity, following the criterion of highest continuity and maximum smoothness. (a) The dashed line perfectly fit data error boundaries with only one surface, but roughness is extremely high, and the principle of highest continuity is violated; conversely, the solid line fits the data also taking into account a priori information on major vertical offsets, following the criterion of highest continuity. Three-dimensional view of the interpolation process with (b) one and (c) two surfaces.

of an interface is achieved by interpolation between observed data. The regions characterized by a complex tectonic setting with several active and ancient suture zones, like the central Mediterranean, usually exhibit large variability of Moho offsets. Such variability must be taken into account in the interpolation process. While small offsets do not force the interpolation surface to lay outside the data error boundaries and thus they may be modeled at the cost of a small increase of the roughness value, very large offsets are usually related to major lithosphere plate or block boundaries and they can't be modeled with a single Moho surface. Hence, their modeling comes at the cost of violating the criterion of highest continuity (see Figure 2a). To account for such first-order Moho offsets, three main surfaces are used to fit the data (see section 2.2 and the polygons drawn in Figure 4) and thus each Moho segment is related to a specific surface based on a priori information.

2.1. Receiver Function

[4] Despite the significant number of CSS investigations performed in and around the Italian peninsula, their distribution is uneven. The Adriatic side of the northern Apennines and the eastern Po plain are poorly covered by CSS experiments. A number of surveys have been performed in the central and southern Apennines but, unfortunately, part of them only enlightens the shallow crust, and no fingerprints of the Moho are visible [*Improta et al.*, 2000; *Scrocca et al.*, 2003; *Patacca and Scandone*, 2007]. Moreover, part of the seismic profiles is either of poor quality or barely useful to reconstruct the Moho topography giving only inferences on a mean 1-D model [*Morelli et al.*, 1977]. Other potentially very important seismic profiles are still under elaboration. The poor coverage by CSS in large parts of the Italian peninsula is a problem addressed by other authors while mapping the Moho topography in the central Mediterranean area [*Geiss*, 1987; *Meissner and Mooney*, 1998; *Du et al.*, 1998; *Marone et al.*, 2003]. Typically, the adopted solution is merging results from CSS exploration with other kind of geophysical information, i.e., from surface waves or gravimetric studies. This approach has been largely used to fill information gaps [*Geiss*, 1987] because it allows obtaining smooth and continuous surfaces. Mixing different kind of geophysical observations and methods, however, reduces consistency and reliability of the results in all regions. To complement CSS observations, maintaining the implicit seismic consistency of the data set, we implemented a method to use results from receiver function (RF) studies by various authors [*Lombardi et al.*, 2008;

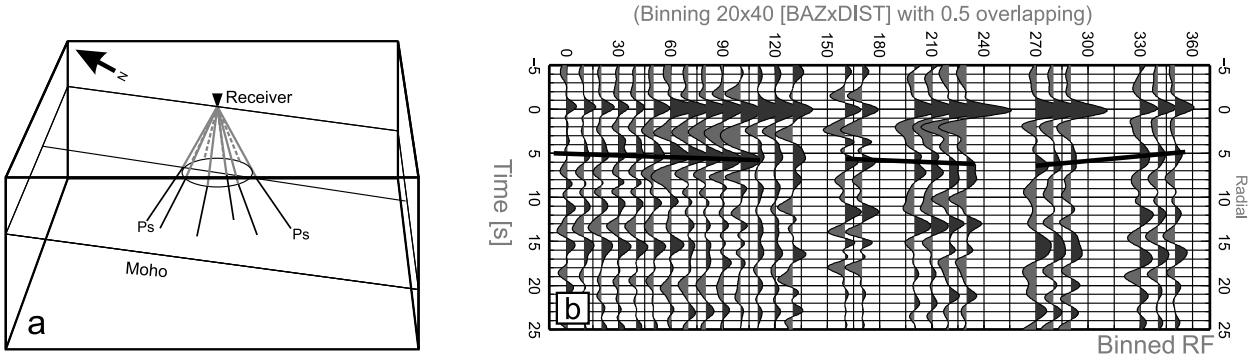

Figure 3. (a) Schematic representation of seismic discontinuity sampling in the receiver function method; Moho sampling is influenced by distribution (delta and azimuth) of teleseismic sources with respect to the receiver (seismic station). (b) Example of back azimuthal sweep for binned receiver functions (radial component). Single RF are binned over 20° of back azimuth and 40° of epicentral distance, with a 50% overlap between adjacent bins: light and dark gray areas represent positive and negative refractions, respectively, at different discontinuities beneath the receiver, while the black thick solid line indicates the Moho feature.

Piana Agostinetti and Amato, 2009; *Geissler et al.*, 2010], similarly to CSS data.

[5] Teleseismic receiver function methods use P to S_V waves converted at sharp seismic discontinuities beneath a receiver (seismic station). These phases are typically better observed at epicentral distances between 35° and 95°, and they appear in the coda of the P wave. Receiver functions are obtained from the broadband seismograms using a time domain deconvolution of the horizontal components (radial and transverse) by the vertical one [*Langston*, 1979] designed to emphasize the presence of P- to S_V-mode conversions. Analysis of the RF is an excellent method to constrain depth and dip of first-order seismic discontinuities beneath three-component seismic stations [*Langston*, 1979; *van der Meijde et al.*, 2003]. For this reason, teleseismic receiver functions are increasingly often used to locally determine depth and dip of crustal and upper mantle discontinuities [*Langston*, 1979; *Owens et al.*, 1984; *Li et al.*, 2000; *Piana Agostinetti et al.*, 2002; *Li et al.*, 2003; *Mele and Sandvol*, 2003; *Margheriti et al.*, 2006].

[6] Figure 3a shows that seismic rays sample the discontinuity within a circular area with radius from 0.4 to 0.75 times its depth [*Langston*, 1979]. Hence, RF supply depth values which are the mean of the Moho depth around the receiver.

[7] Since the method by *Waldhauser* [1996] needs 2-D profiles to work, we made the choice to represent Moho depth from the RF as the diameter of the circular area. As for the size of the diameter we made a general choice of 20 km width that is conservative (i.e., not overestimating the precision of the measure) respect to Moho depths in Italy ranging from a 10–20 km (Tyrrhenian plate, minimum radius = 4 km) to 35–50 km (Adriatic plate and European plate, maximum radius = 38 km). Estimated errors in the depth determinations are usually within ±5 km, depending on the quality of the waveforms, the completeness of the data set (events' azimuth and distance distribution), and the complexity of the lithosphere structure beneath the receiver.

[8] We then attributed to each datum the three different weights, following this criterion: W_Q for the data quality and number of RFs forming the single data set (Figure 3b); W_C for the error depth (following the scheme reported in Table 1), and W_T (type) usually set to 1.0 since high to mean quality azimuthal coverage ensures at least bidirectional sampling of the discontinuity. Finally, according to the geographic location we attributed the station to one of the three polygons of Figure 4 that outline the range of the different Moho surfaces (see next chapter for details).

2.2. Moho Interpolation Polygons

[9] In the past years, surface geology studies, CSS experiments, high-resolution tomography, and receiver function analysis demonstrated that prominent suture zones and large vertical Moho offsets exist in the central Mediterranean region and represent the boundaries between three main lithospheric units. The boundary between the European plate and the Adriatic plate is found beneath the Alpine belt, along the Insubric Line suture zone and the western margin of the Ivrea Verbano Body

Table 1. Scheme for W_C Values Conversion to Moho Depth Uncertainties From RF Data

ε Depth (km)	W_C
0 – ±1	1.0
±1 – ±2	0.8
±2 – ±4	0.4
±4 – ±8	0.2
>±8	0.0

[*Solarino et al.*, 1996, 1997; *Schmid et al.*, 2004] (see Figure 1). The southern part of the EGT profile [*Ye et al.*, 1995] clearly shows the shallow Tyrrhenian Moho overlaying the southward dipping Adriatic Moho beneath the Ligurian Alps (see Figure 1). Based on such a priori information, *Waldhauser et al.* [1998] defined three different interpolation surfaces for the Adriatic, the European, and the Tyrrhenian Moho, respectively (see Figure 4), thus following the criteria of "highest continuity–least roughness" and also taking into account important first-order features of the regional geodynamic setting. We include in our model the Italian Peninsula, from the northern Apennines to the Calabrian Arc, Sicily, Corsica-Sardinia, and the Tyrrhenian, Adriatic, and Ionian Sea. The boundary between the Tyrrhenian plate and the Adriatic plate, defined by *Waldhauser et al.* [1998, 2002], stops southward at 43°N, in correspondence with the transition between the western Alps and the northern Apennines (see Figure 1). Evidence from controlled source seismic surveys [*Ponziani et al.*, 1995; *Barchi et al.*, 1998; *Ponziani et al.*, 1998; *De Franco et al.*, 2000; *Finetti et al.*, 2001; *Scrocca et al.*, 2003] and RF analysis [*Levin et al.*, 2002; *Piana Agostinetti et al.*, 2002; *Mele and Sandvol*, 2003; *Margheriti et al.*, 2006; *Bianchi et al.*, 2008; *Di Bona et al.*, 2008; *Roselli et al.*, 2008; *Bianchi et al.*, 2010], performed in the past years in the northern Apennines, reveal the southward continuation of the large vertical Moho

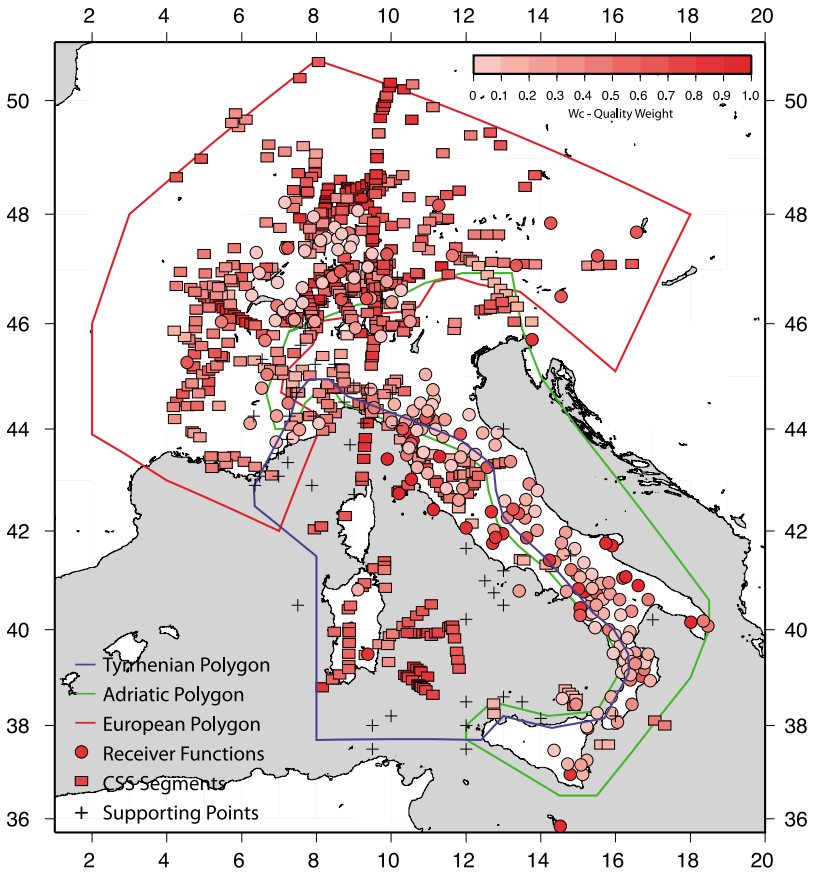

Figure 4. Geometry of the polygons defining the limits of the three Moho surfaces and RF and CSS segments used to generate the map; the external limits exceed the interpolated volume, while within the sampled volume the plate boundaries are defined based on geologic and geophysics information. In particular, the plate boundary at Moho depth between the Tyrrhenian lithosphere and the Adriatic lithosphere is redrawn from *Di Stefano et al.* [2009]. The ~3000 CSS and RF segments used to build the Moho map are represented by solid rectangles and solid circles, respectively. Red tones are related to the quality estimation.

offset separating the shallow Tyrrhenian Moho from the southwestward dipping Adriatic Moho. Results from recent high-resolution seismic tomography [*Di Stefano et al.*, 2009] confirm this evidence and allow tracing the Adriatic-Tyrrhenian plate boundary from the northern Apennines to the Calabrian Arc and eastern Sicily (see Figure 1). The Adriatic surface in the present paper also includes the Ionian Moho (see Figure 4), because evidence for seismically active plate margins or large vertical Moho offsets separating the Adriatic from the Ionian-African plate are missing [*Chiarabba et al.*, 2005]. Similarly we relate Moho segments pertaining to the Corsica-Sardinia lithosphere to the Tyrrhenian plate, though from the geological and the geodynamical points of view, Corsica-Sardinia was part of the Eurasian plate before its counterclockwise rotation [*Faccenna et al.*, 2002; *Speranza and Chiappini*, 2002]. Hence the Tyrrhenian plate is here intended from the Ligurian Sea to the southern Tyrrhenian Sea and from the western side of the Italian peninsula to the Corsica-Sardinia block (see Figure 1).

3. Data Set

[10] In Figure 4 we also show the weights of the Moho data introduced in the present work, together with those by *Waldhauser et al.* [1998]. Additional data represent more than half of our complete data set. During the past 40 years, the central Mediterranean has been intensively probed by CSS exploration, both with local-scale surveys and by regional-scale long-term projects like the CROP [*Scrocca et al.*, 2003]. Large amounts of seismic data regarding the deep structure and the Moho depth have been acquired since 1950 [*Maistrello and Musacchio*, 2003]. In the Alpine region, over 200 reversed and unreversed refraction profiles, 25 fan, and 30 near vertical profiles were compiled and referenced by *Waldhauser et al.* [1998], including EGT [*Ye et al.*, 1995], ECORS [*Nicholas et al.*, 1991; *Bernabini et al.*, 2003], and TRANSALP [*TRANSALP Working Group*, 2002; *Castellarin et al.*, 2003]. In this work we focus on the Italian peninsula, Corsica, Sardinia, Sicily, and the surrounding seas. In the northern Apennines, Moho topography has been revealed by the Near Vertical Reflection (NVR) CROP03 profile [*Pialli et al.*, 1998] and by a number of Wide-angle Refraction (WAR) both reversed and unreversed profiles [*Ponziani et al.*, 1995; *Barchi et al.*, 1998; *De Franco et al.*, 1998; *Ponziani et al.*, 1998]. The LISA and CROP Mare II projects [*De Franco et al.*, 2000; *Scrocca et al.*, 2003], performed in the Tuscan-Latium peri-Tyrrhenian area, the southern part of the long-range EGT profile, and the many short local transverse CSS profiles [*Egger*, 1992] complement the information about the crustal structure and the Moho topography beneath the Ligurian Sea and the northern Tyrrhenian Sea and beneath Corsica and Sardinia. Again, in the framework of the "CROP Mare II," wide-angle seismic profiles give local insights on the crustal structure of the southern Tyrrhenian Sea, the Sicily channel, and the Adriatic Sea [*Chironi et al.*, 2000]. In the Tyrrhenian Sea, only few publications show ray tracing and original waveform traces that are needed to define error boundaries and to weight data. In our map we introduce important new original information from several CSS profiles held in the southwestern Tyrrhenian Sea from *Carrara* [2002], thus filling a large gap. Such data occupy a key position in the central western Mediterranean, being located between Sardinia and the Maghrebian chain of Tunisia and Sicily, bounded to the north by the Orosei Canyon (see Figure 1). The high-resolution multichannel seismic profiles (MCS, near 2000 km), previously acquired by French and Italian groups, have been reprocessed by *Carrara* [2002] to obtain important deep information regarding the nature and distribution of continental and oceanic crust, and to identify Moho depth. The seismic stratigraphy, and hence the P wave velocities, along the selected profiles have been constrained by laterally extrapolating information from nearby drillings of the ODP Leg 107 (see Figure 1), decisive for the stratigraphic-tectonic interpretation of the investigated area [*Kastens et al.*, 1987, 1990]. In the remaining portion of the southern Tyrrhenian, only author's interpretation is available at present. The depth of the Moho beneath Italy has been investigated before with receiver functions for restricted areas, by various authors following different inversion methodologies, scales and targets for the studies [*Piana Agostinetti et al.*, 2002; *Mele et al.*, 2006; *Bianchi et al.*, 2008; *Di Bona et al.*, 2008; *Roselli et al.*, 2008; *Piana Agostinetti and Amato*, 2009; *Bianchi et al.*, 2010]. To build a complete and homogeneous high-quality data set, we used results from three works, in which the Zhu-Kanamori method (ZK) [*Zhu and Kanamori*, 2000] has been applied to determine the crustal thicknesses for portions of Italy, and to map out the lateral variation of Moho depth.

[11] The ZK method gives well-constrained measures, with error assessment based on the Taylor expansion of the stacking function of thickness and V_P/V_S ratio. In addition to the standard ZK

approach, *Piana Agostinetti and Amato* [2009] perform several inversions following the bootstrap approach and taking the minimum-maximum depths as error boundaries. A reference V_P of 6.5 km/s has been used which is a good estimate of average crustal P wave velocity in Italy by local earthquake tomography [*Di Stefano et al.*, 2006, 2009]. Obviously, strong local 3-D velocity variations including sedimentary basins and lower crustal wedging will have an effect on RF-based Moho depth estimations. In many cases, however, such 3-D velocity effects are also visible in azimuthally well-sampled RF and, therefore, they are included in our uncertainty estimates for Moho depth. Significant similar effects on all azimuths may only go undetected in very large and deep sedimentary basin such as the Po plain where our Moho map is mainly based on CSS information. All the papers furnish a standard deviation as the final depth error estimation. Crustal thicknesses are estimated from the delay time of the Moho P- to S_V-converted phase and the later multiple converted phases.

[12] The receiver function studies selected for the present paper allow reducing small (northern Apennines) to large (southern Apennines) gaps in peninsular Italy [*Piana Agostinetti and Amato*, 2009], western and central Alps [*Lombardi et al.*, 2008], and eastern Alps [*Geissler et al.*, 2010] with high-quality observations at a large number of seismic stations. An ensemble of 226 Moho depths underneath the respective seismic stations composes the resulting data set. In the southeastern Tyrrhenian region and in the Adriatic region, where the absence of constrainable information might induce numeric instabilities in the interpolation process, we introduce "supporting points." The supporting points are values of Moho depth that help to fill gaps inside or at the edge of the Moho polygons. Such values cannot be introduced into the data set due the impossibility to assess associated errors. These points are derived from literature by selecting RF or CSS studies for which authors do not publish related original data.

[13] For the Adriatic region we extracted information from CSS studies by *Dragasevic* [1969]. For the Tyrrhenian region not covered by *Carrara* [2002] we use *Sartori et al.* [2004] and other seismological information [*Steinmetz et al.*, 1983; *Kastens et al.*, 1987; *Sartori et al.*, 1989; *Kastens et al.*, 1990].

[14] The final *RMS* (Root Mean Square) for the interpolated surfaces, synthetically representing the level of misfit for the European, Adriatic, and Tyrrhenian Moho, is very low being 1.4 km, 3 km, and 2 km, respectively. Conversely, interpolating the same data with only one surface gives a final *RMS* of 3.6 km. These values support the choice of including plate boundaries, namely three different surfaces, as a priori information.

[15] In Figure 5 we present details on the depth misfit in km, between real data and the final surfaces. As shown in Figure 5a, misfit is lower than ±5 km, ±2 km, and ±1 km for ~94%, ~74%, and ~50% of the data set respectively. The map view of the distribution of the depth misfit (Figure 5b) clearly shows that the highest misfit values correspond to boundary areas where the curvature of the Moho is stronger. Anyway such higher values are generally smaller than ±6 km. This analysis demonstrates that the final interpolated map is well constrained, with data misfit largely within the error boundaries expected for CSS and RF methods, thus giving a suitable image of the Moho surface and of the offset at the plate boundaries between the three lithospheres.

4. The Moho Map

[16] In Figure 6 we show the results of the 3-D interpolation for the Adriatic, the Tyrrhenian, and the European Moho.

[17] The main feature of the Moho in the central Mediterranean region is the variability of its topography. This is a dominant characteristic not only at the boundaries between the three interacting lithospheres, where large vertical offsets are revealed by seismic exploration and modeled by our interpolation method, but also within each plate, where Moho depth varies within a range of ~50 to ~10 km, indicating significant ongoing tectonic activity. Details about the European Moho beneath the Alps are given by *Waldhauser et al.* [1998, 2002]. We here focus on the Tyrrhenian Sea, and insular and peninsular Italy.

[18] The Tyrrhenian Moho shows a much shallower mean depth with respect to the ~32 km of an average continental crust [*Mueller*, 1977; *Holliger and Kissling*, 1992].

[19] Minimum depths are imaged in the central Tyrrhenian sea (from 20 km to 10 km depth) where the Seamount Marsili volcano is located [*Sartori et al.*, 1989; *Marani and Trua*, 2002]. Rheologically weak lithosphere in this region was affected by high extensional rates [*Faccenna et al.*, 1997; *Panza et al.*, 2003]. The extension appears to be accomplished

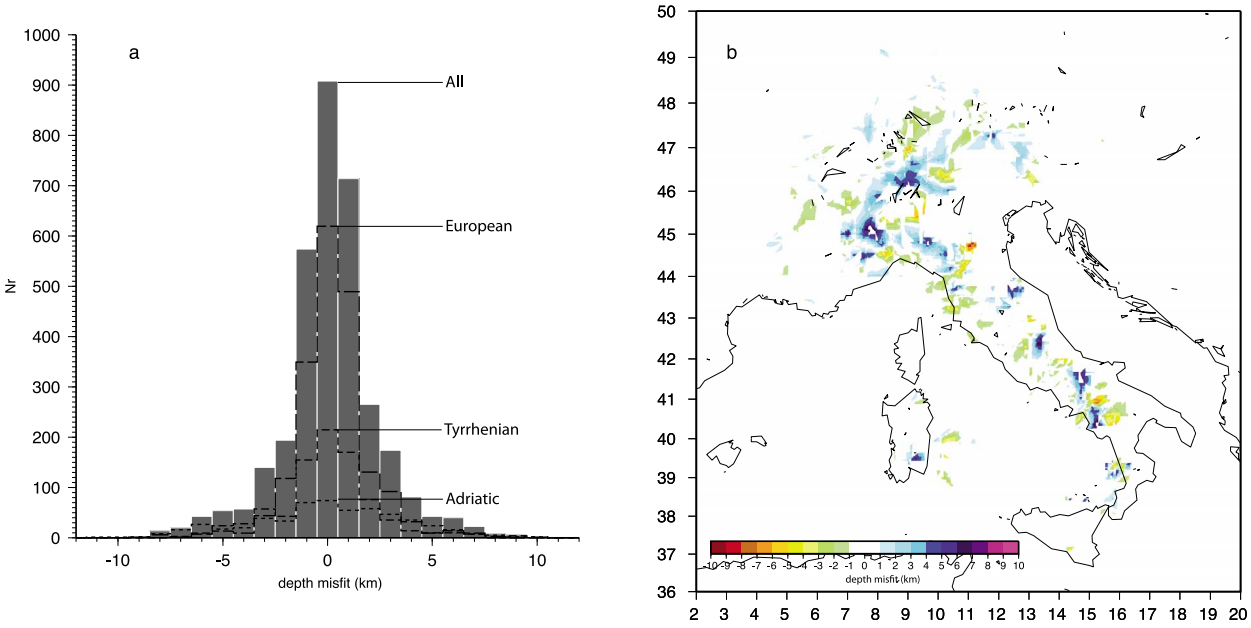

Figure 5. (a) Distribution of the misfit (km), between the observed and the interpolated depths in correspondence of each data point; (b) map view of the misfit distribution.

by crustal thinning and linked to a quick mantle exhumation process as testified by sepentinized peridotites drilled beneath 136 m at ODP Site 651 (Figure 1) in the middle of the Vavilov basin [*Bonatti et al.*, 1990].

[20] The Tyrrhenian plate includes slivers of regular and thinned lithosphere of both continental and oceanic origin affected by extensional tectonics due to the opening of the Tyrrhenian Sea (since 12 My ago). Specifically, the southern basin is floored by lithosphere at different stages of tectonic evolution and petrographic composition, while the northern part and the coastal regions are mainly floored by thinned continental crust [*Duschenes et al.*, 1986; *Sartori et al.*, 2001; *Nicolosi et al.*, 2006].

[21] A gentle deepening of the Moho discontinuity marks the transition to the coastal areas [*Locardi and Nicolich*, 1988; *Egger*, 1992; *Ventura et al.*, 1999; *Chironi et al.*, 2000; *Sartori et al.*, 2001].

[22] The depth of the Moho increases toward the Corsica-Sardinia block (25 km to 32 km), toward the Aeolian Arc (19–20 km) and toward the Apennines belt. The Corsica-Sardinia block rotated and translated away from Europe in the wake of the retreating Ionian slab. Its characteristics are those of a normal continental lithosphere with Moho depth undulations around 30 km. Thus from Corsica and Sardinia to the East and to the Southeast, a generalized thinning of the crust is observed. Northward from Corsica to the western Alps, the Ligurian Sea has been characterized by the evolution from normal to extended thin continental crust and by the strong influence of asthenospheric intrusions [*Egger*, 1992; *Makris et al.*, 1999]. North of the 41° of latitude to the Ligurian Sea our map shows two minima south and north of the Elba Island, with depths ranging from 22 km to 15 km respectively.

[23] *Carrara* [2002] and *Sartori et al.* [2001, 2004] showed that the opening of the Tyrrhenian sea started in Upper Tortonian times (~7.3 Ma) with a consistent crustal thinning in the Cornaglia Terrace and a confined steep mantle uprise from the Sardinia continental block toward the Vavilov basin. In addition, the crustal discontinuity named OCL transfer zone (Figure 1) seems to influence the Moho distribution. This probably Mesozoic lineament [*Sartori et al.*, 2001, 2004] trends roughly E-W, almost along the 40°N parallel. During lower and middle Miocene times it was reactivated as a transfer zone separating the thick (~50 km) deformed "Alpine" crust (north of Orosei canyon) from the moderately deformed Ercinian crust toward south.

[24] Such uprise continues on to the center of the Tyrrhenian Basin where, in the western Vavilov plain, the mantle outcrops [*Kastens et al.*, 1987, 1990]. Eastward, a consistent vertical offset and a partial overlapping mark the border with the Adriatic Moho [*Ponziani et al.*, 1995; *Barchi et al.*, 1998; *De Franco et al.*, 1998; *Pauselli et al.*, 2006; *Di Bona et al.*, 2008; *Roselli et al.*, 2008; *Piana*

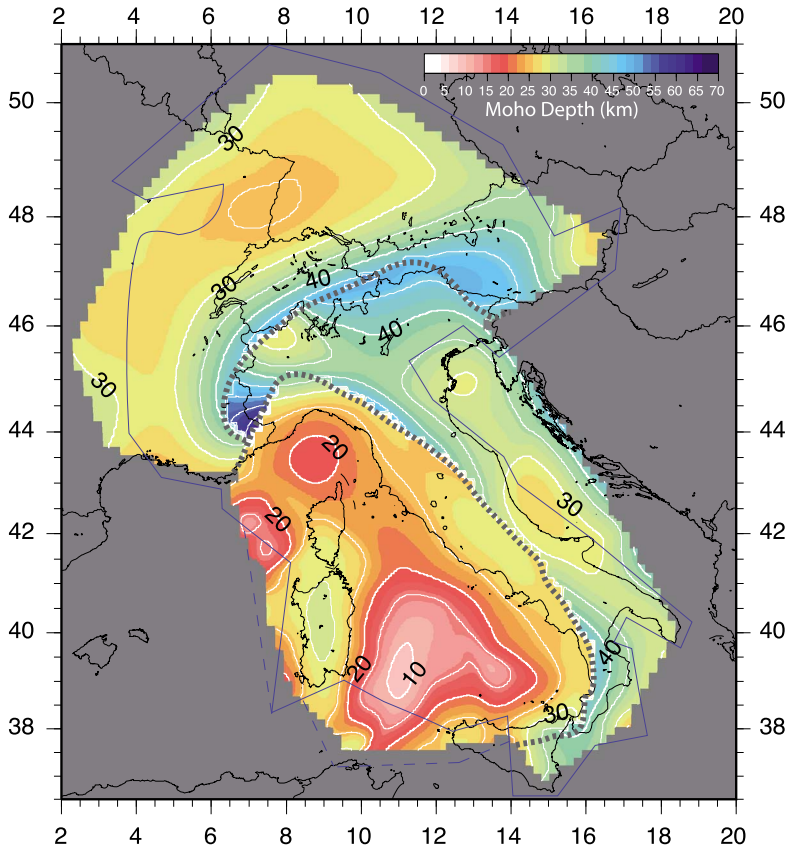

Figure 6. Map and contour lines describing the Moho topography for the European, Adriatic, and Tyrrhenian plate units. Contour lines are drawn with thick and thin white lines every 10 and 5 km depth steps, respectively. The dashed gray line represents the plate boundary. The solid blue line encloses the real data area. The dashed blue line includes external supporting points. Outside the blue lines, values are due to interpolation effects.

Agostinetti and Amato, 2009; *Bianchi et al.*, 2010]. The Adriatic plate as we define it here, includes the Ionian lithosphere, subducting beneath the Tyrrhenian plate in the Calabrian Arc. Adriatic continental lithosphere sensu stricto shows a mean Moho depth of about 30–35 km, typical of a normal continental crust, only beneath the Adriatic sea. In fact the Adriatic Moho deepens down to 40–50 km depth toward the Tyrrhenian plate southwestward and northwestward along the Apennines belt and the Calabrian Arc, respectively. The NW-SE trending bulge modeled beneath the Adriatic Sea, between the eastward and westward plunging branches of the Adriatic plate (see Figures 6 and 7 and *Di Stefano et al.* [2009]), shows prominent undulations along the peninsula, especially at the boundary where the Adriatic plate underthrusts the Tyrrhenian plate [*Steckler et al.*, 2008; *Di Stefano et al.*, 2009; *Piana Agostinetti and Amato*, 2009].

[25] Greater depths at the boundary characterize the northern Apennines and the Calabrian Arc, while shallower depths characterize the central and southern Apennines, and the western Po plain. Moreover, the steepness of Adria at the plate boundary approximately decreases from north to south.

[26] To better describe the relationship between the Tyrrhenian, the Adriatic, and the European Moho along their respective plate boundaries, we plot in Figure 7 eleven vertical sections showing the Moho in comparison with topography and Bouguer gravity anomalies [*Consiglio Nazionale delle Ricerche*, 1991]. The broad trend of gravity anomalies depends mainly on Moho topography and on density variations in the uppermost crust.

[27] Their distribution gives a measure of mass excess or deficit beneath the foredeep basin and adjacent thrust belt. It reflects the contribution of topography and bathymetry and the density contrast between crust and mantle across the deflected Moho [*Royden*, 1988]. Moving from south to north, the profiles show increasing negative anomalies due to the progressive thickening of the sedimentary layers, in particular the foredeep Po basin [*Royden*, 1988; *Holliger and Kissling*, 1992].

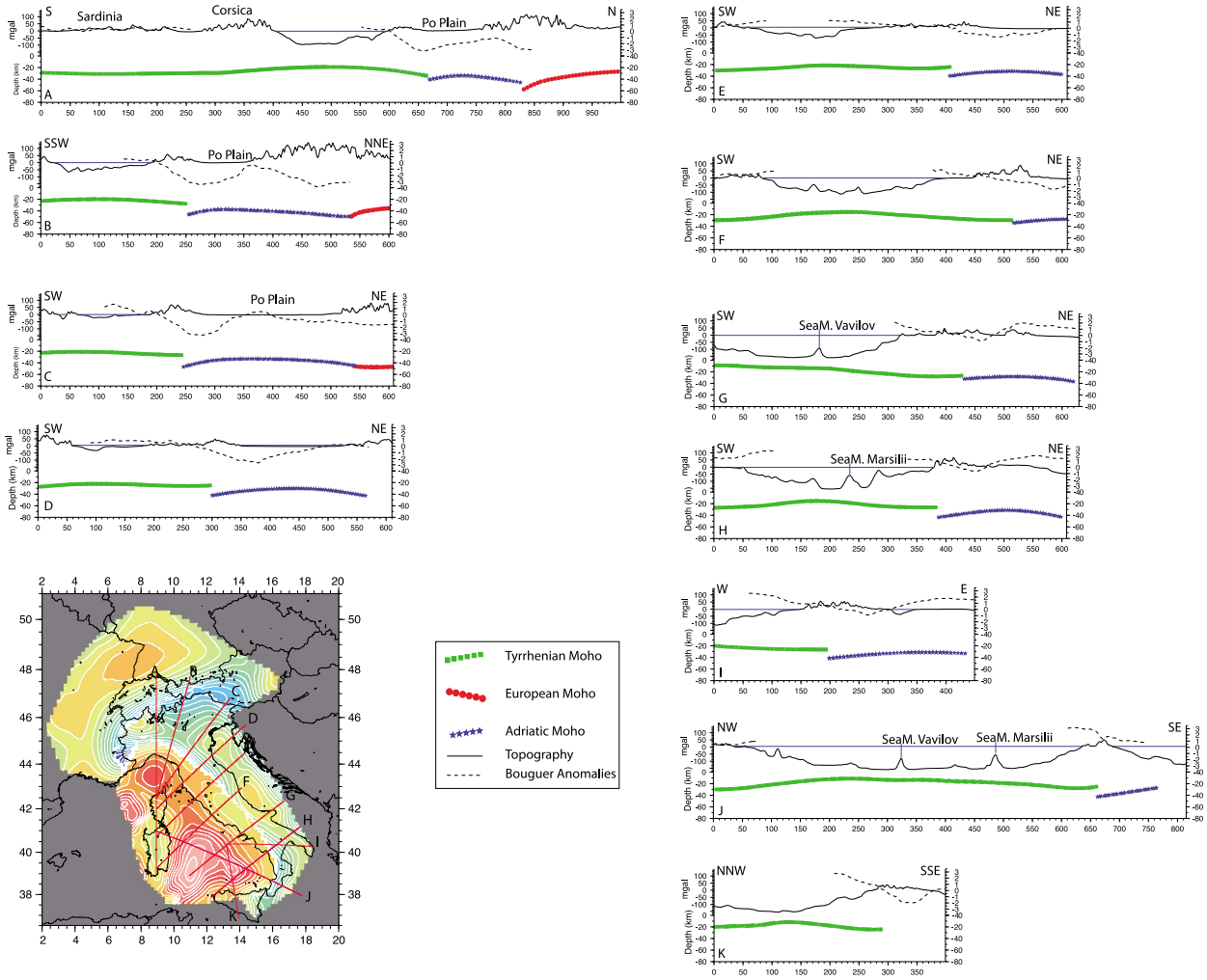

Figure 7. Vertical section through the obtained Moho map; in red, green, and blue we report the depths of the European, Tyrrhenian, and Adriatic Moho, respectively. In the inset map we report the traces of the vertical sections over the Moho topography; vertical section A is cut along the EGT seismic profile [*Ye et al.*, 1995], while vertical sections D and E are cut close to the CROP03 profile [*Pialli et al.*, 1998].

[28] The European and the Adriatic Moho show a significant vertical offset (section A) in the western part and a small (section B) to no offset (section C) beneath the Alpine belt. Similarly, the offset between the Adriatic Moho, gently plunging toward the south and southwest, and the Tyrrhenian Moho, varies from beneath the northern Apennines (section C) to the Calabrian Arc (section J) along the Italian peninsula.

[29] While the depth difference at plate boundary is about 15–20 km beneath the northern Apennines (sections C to E) and beneath the Calabrian Arc (H-J), it strongly decreases to only about 5 km beneath the central and southern Apennines (sections F and G), confirming the strong lateral variability of the shallow subduction geometry beneath Italy discussed by *Di Stefano et al.* [2009].

[30] We observe in all profiles the minimum gravimetric zones shifted to NE with respect to both the Apennine chain and the plate boundary at Moho depth. Though the trend of Bouguer gravity anomalies cannot directly be related to plate deflection [see, e.g., *Kissling*, 1993], it is worth noting how well negative anomalies, indicating the presence of relatively lower-density material, correspond to the location of the plate boundary beneath Italy. The source for the low-frequency anomaly is likely related to deep crustal material resulting from Adriatic Moho flexing.

5. Discussion and Conclusions

[31] We present a new map of the Moho topography for the Italian region, obtained by integrating

weighted CSS and receiver function data. The *Waldhauser et al.* [1998] procedure, previously applied to the Alpine region, has been modified to include, along with CSS data, Moho depths from receiver function analysis. The joint use of such information allows us to increase the resolution of the Moho topography, laterally averaging 2-D results from active seismic profiles and 1-D results from receiver function. This implementation has large benefit in areas where deep controlled source seismic data are lacking or incomplete and it allows us obtaining a more homogeneously sampled and well constrained image of the Moho topography in the study region. In fact, thanks to our implementation we were able to extend the consistency of the adopted method to the constantly increasing data set of receiver functions.

[32] Though in some areas, like the Adriatic Sea and the Southeastern Tyrrhenian Sea, more high-quality information on the Moho depth are needed to better constrain our interpolation results, we consider our map an important step forward with respect to previous Moho maps for the same area, because it includes a much larger and consistent set of receiver function information, with a very good fit of data obtained by the application of the "highest continuity–least roughness" principle (see section 2.2).

[33] The map shows large lateral heterogeneity of the Moho depth and a complex interaction between the three main plates, confirming results from high-resolution P wave seismic tomography. Such medium- to high-frequency undulations probably reflect heterogeneities inherited from the former Adriatic continental margin [*Di Stefano et al.*, 2009, and references therein]. The complex tectonics since late Cretaceous modeled the continental or partially oceanic (i.e., the central southern Tyrrhenian) crust, creating the imaged lateral undulation of the Moho topography. Tethys subduction and the subsequent continental collision created a deflection of the European and Adriatic crust down to 40–50 km in the Alps. As a consequence of the Apennines subduction, the Adriatic continental crust underthrusted the Tyrrhenian plate, reaching depths of about 40–50 km and 30–40 km, at the plate boundary, in the northern and central southern Apennines respectively. In the Apennines, the steepness of the Adriatic Moho slightly decreases southward, suggesting that the past 20 Myr subduction/collision process was not uniform along the belt.

[34] Thus, the offset of the Moho depth, imaged nearby the plate boundary between the Tyrrhenian and the Adriatic plates, is smaller in the central southern Apennines, while it is more pronounced in the northern Apennines and in the Calabrian Arc. These features are exemplified in Figure 7 in which we report vertical sections cut through the Moho map along representative profiles. Crustal seismicity, confined above 20 km depth, and the entire Apennines normal faulting belt are located above this plate boundary [*Chiarabba et al.*, 2005], in a region where the Adriatic Moho reaches the maximum depths.

[35] The Moho depth revealed beneath the Tyrrhenian Sea, varying from 10 to 12 km in the southern Tyrrhenian to 20 km in the Ligurian Sea and to 30 km beneath Corsica-Sardinia, marks the transition from extremely to moderately stretched continental lithosphere and to normal continental lithosphere, respectively. These differences highlight the different stages of evolution of the Tyrrhenian Sea opening.

[36] The one we presented in this work is the most complete and consistent Moho map that is available at present for the Italian region. Furthermore, based on the method we used and the implementation we described previously, it can be easily updated when more receiver function or CSS data will be available in the near future. We propose the present release as a well-constrained reference model of the Moho for high-resolution geophysical studies on the crustal structure and the geodynamics of the target region.

Acknowledgments

[37] The authors would like to thank M. Grad and J. Plomerová for their detailed and constructive review of our paper. Their comments and suggestions allowed us to better expound our method and results and to improve the readability of our paper. We are also grateful to F. P. Lucente for his preliminary revision and to N. P. Agostinetti and A. Amato for providing us with teleseismic receiver function original data for the Italian Seismic Network.

References

Barchi, M., G. Minelli, and G. Pialli (1998), The CROP 03 profile: A synthesis of results on deep structures of the northern Apennines, *Mem. Soc. Geol. Ital.*, *52*, 383–400.

Baumann, M. (1994), Three-dimensional modeling of the crust-mantle boundary in the Alpine region, Ph.D. thesis, Swiss Fed. Inst. of Technol., Zurich, Switzerland.

Bernabini, M., R. Nicolich, and R. Polino (2003), Seismic lines CROP-ECORS across the western Alps, *Mem. Desc. Carta Geol. Ital.*, *62*, 89–95.

Bianchi, I., N. Piana Agostinetti, P. De Gori, and C. Chiarabba (2008), Deep structure of the Colli Albani volcanic district (central Italy) from receiver functions analysis, *J. Geophys. Res.*, *113*, B09313, doi:10.1029/2007JB005548.

Bianchi, I., J. Park, N. Piana Agostinetti, and V. Levin (2010), Mapping seismic anisotropy using harmonic decomposition of receiver functions: An application to northern Apennines, Italy, *J. Geophys. Res.*, *115*, B12317, doi:10.1029/2009JB007061.

Bonatti, E., M. Seyler, J. E. T. Channell, J. Giraudeaud, and G. Mascle (1990), Peridotites drilled from the Tyrrhenian Sea, ODP Leg 107, *Proc. Ocean Drill. Program Sci. Results*, *107*, 37–47.

Capitanio, F., and S. Goes (2006), Mesozoic spreading kinematics: Consequences for Cenozoic central and western Mediterranean subduction, *Geophys. J. Int.*, *165*, 804–816, doi:10.1111/j.1365-246X.2006.02892.x.

Carrara, G. (2002), Evoluzione cinematica neogenica del margine occidentale del bacino tirrenico, Ph.D. thesis, Parma Univ., Parma, Italy.

Castellarin, A., et al. (2003), The trans-Alp seismic profile and the CROP 1-a subproject, *Mem. Desc. Carta Geol. Ital.*, *62*, 107–126.

Catalano, R., C. Doglioni, and S. Merlin (2001), On the Mesozoic Ionian basin, *Geophys. J. Int.*, *144*, 49–64, doi:10.1046/j.0956-540X.2000.01287.x.

Chiarabba, C., L. Jovane, and R. Di Stefano (2005), A new global view of Italian seismicity using 20 years of instrumental recordings, *Tectonophysics*, *395*, 251–268, doi:10.1016/j.tecto.2004.09.013.

Chironi, C., L. D. Luca, I. Guerra, D. Luzio, A. Moretti, and M. Vitale (2000), Crustal structures of the southern Tyrrhenian Sea and the Sicily Channel on the basis of the m25, m26, m28, m39 WARR profiles, *Bol. Soc. Geol. Ital.*, *119*, 189–203.

Consiglio Nazionale delle Ricerche (1991), Structural model of Italy and gravity map, Rome.

De Franco, R., F. Ponziani, G. Biella, G. Boniolo, G. Caielli, A. Corsi, M. Maistrello, and A. Morrone (1998), DSS-WAR experiment in support of the CROP-03 project, *Mem. Soc. Geol. Ital.*, *52*, 67–90.

De Franco, R., G. Biella, G. Caielli, A. Corsi, A. Mauffret, I. Contrucci, and A. Nercessian (2000), Interpretation of wide angle reflection refraction data in the Tuscan-Latium peri-Tyrrhenian area, *Bol. Soc. Geol. Ital.*, *119*, 171–188.

Dézes, P., and P. A. Ziegler (2001), European map of the Mohorovičić discontinuity, paper presented at 2nd EUCOR-URGENT Workshop (Upper Rhine Graben Evolution and Neotectonics), Mt. St. Odile, France.

Di Bona, M., F. P. Lucente, and N. Piana Agostinetti (2008), Crustal structure and Moho depth profile crossing the central Apennines (Italy) along the N10° parallel, *J. Geophys. Res.*, *113*, B12306, doi:10.1029/2008JB005625.

Di Stefano, R., F. Aldersons, E. Kissling, P. Baccheschi, C. Chiarabba, and D. Giardini (2006), Automatic seismic phase picking and consistent observation error assessment: Application to the Italian seismicity, *Geophys. J. Int.*, *165*, 121–134, doi:10.1111/j.1365-246X.2005.02799.x.

Di Stefano, R., E. Kissling, C. Chiarabba, A. Amato, and D. Giardini (2009), Shallow subduction beneath Italy: Three-dimensional images of the Adriatic European-Tyrrhenian lithosphere system based on high-quality P wave arrival times, *J. Geophys. Res.*, *114*, B05305, doi:10.1029/2008JB005641.

Doglioni, C., and E. Carminati (2002), The effects of four subductions in the NE-Italy, *Mem. Soc. Geol. Ital.*, *54*, 1–4.

Dragasevic, T. (1969), Investigation of the structural characteristics of the Mohorovicic discontinuity in the area of Yugoslavia, *Bol. Geofis. Teor. Appl.*, *11*, 57–69.

Du, Z., A. Michelini, and G. Panza (1998), EurId: A regionalized 3-D seismological model of Europe, *Phys. Earth Planet. Inter.*, *106*, 31–62, doi:10.1016/S0031-9201(97)00107-6.

Duschenes, J., M. Sinha, and K. Louden (1986), A seismic refraction experiment in the Tyrrhenian Sea, *Geophys. J. Int.*, *85*, 139–160, doi:10.1111/j.1365-246X.1986.tb05175.x.

Egger, A. (1992), Lithospheric structure along a transect from the northern Apennines to Tunisia derived from seismic refraction data, Ph.D. thesis, Swiss Fed. Inst. of Technol., Zurich, Switzerland.

Faccenna, C., P. Davy, J. Brun, R. Funiciello, D. Giardini, M. Mattei, and T. Nalpas (1996), The dynamics of back-arc extension: An experimental approach to the opening of the Tyrrhenian Sea, *Geophys. J. Int.*, *126*, 781–795, doi:10.1111/j.1365-246X.1996.tb04702.x.

Faccenna, C., M. Mattei, R. Funiciello, and L. Jolivet (1997), Styles of back-arc extension in the central Mediterranean, *Terra Nova*, *9*(3), 126–130, doi:10.1046/j.1365-3121.1997.d01-12.x.

Faccenna, C., F. Speranza, F. D. Caracciolo, M. Mattei, and G. Oggiano (2002), Extensional tectonics on Sardinia (Italy): Insights into the arc-back-arc transitional regime, *Tectonophysics*, *356*, 213–232, doi:10.1016/S0040-1951(02)00287-1.

Finetti, I., M. Boccaletti, M. Bonini, A. D. Ben, R. Geletti, M. Pipan, and F. Sani (2001), Crustal section based on CROP seismic data across the north Tyrrhenian-northern Apennines-Adriatic Sea, *Tectonophysics*, *343*, 135–163, doi:10.1016/S0040-1951(01)00141-X.

Geiss, E. (1987), A new compilation of crustal thickness data for the Mediterranean area, *Ann. Geophys., Ser. B*, *5*, 623–630.

Geissler, W., F. Sodoudi, and R. Kind (2010), Thickness of the central and eastern European lithosphere as seen by S receiver functions, *Geophys. J. Int.*, *181*, 604–634, doi:10.1111/j.1365-246X.2010.04548.x.

Grad, M., T. Tiira, and the ESC Working Group (2009), The Moho depth map of the European Plate, *Geophys. J. Int.*, *176*, 279–292, doi:10.1111/j.1365-246X.2008.03919.x.

Holliger, K., and E. Kissling (1992), Gravity interpretation of a unified 2-D acoustic image of the central Alpine collision zone, *Geophys. J. Int.*, *111*, 213–225, doi:10.1111/j.1365-246X.1992.tb00571.x.

Improta, L., G. Iannaccone, P. Capuano, A. Zollo, and P. Scandone (2000), Inferences on the upper crustal structure of the southern Apennines (Italy) from seismic refraction investigation and subsurface data, *Tectonophysics*, *317*, 273–298, doi:10.1016/S0040-1951(99)00267-X.

Kastens, K., et al. (1987), *Proceedings of the Ocean Drilling Program, Initial Reports*, vol. 107, Ocean Drill. Program, College Station, Tex.

Kastens, K., et al. (1990), *Proceedings of the Ocean Drilling Program, Scientific Results*, vol. 107, Ocean Drill. Program, College Station, Tex.

Kissling, E. (1993), Deep structure of the Alps: What do we really know?, *Phys. Earth Planet. Inter.*, *79*, 87–112, doi:10.1016/0031-9201(93)90144-X.

Kissling, E., J. Ansorge, and M. Baumann (1997), Methodological considerations of 3-D crustal structure modeling by 2-D seismic methods, in *Results of NRP 20: Deep Structure of the Swiss Alps*, edited by O. A. Pfiffner, et al., pp. 31–38, Birkhäuser, Basel, Switzerland.

Langston, C. (1979), Structure under Mount Rainier, Washington, inferred from teleseismic body waves, *J. Geophys. Res.*, *84*, 4749–4762, doi:10.1029/JB084iB09p04749.

Levin, V., L. Margheriti, J. Park, and A. Amato (2002), Anisotropic seismic structure of the lithosphere beneath the Adriatic coast of Italy constrained with mode-converted body waves, *Geophys. Res. Lett.*, *29*(22), 2058, doi:10.1029/2002GL015438.

Li, X., S. Sobolev, R. Kind, X. Yuan, and C. Estabrook (2000), A detailed receiver function image of the upper mantle discontinuities in the Japan subduction zone, *Earth Planet. Sci. Lett.*, *183*, 527–541, doi:10.1016/S0012-821X(00)00294-6.

Li, X., G. Bock, A. Vadis, R. Kind, H. Harjes, W. Hanka, K. Wylegalla, M. van der Meijde, and X. Yuan (2003), Receiver function study of the Hellenic subduction zone: Imaging crustal thickness variations and the oceanic Moho of the descending African lithosphere, *Geophys. J. Int.*, *155*, 733–748, doi:10.1046/j.1365-246X.2003.02100.x.

Lippitsch, R., E. Kissling, and J. Ansorge (2003), Upper mantle structure beneath the Alpine orogen from high-resolution teleseismic tomography, *J. Geophys. Res.*, *108*(B8), 2376, doi:10.1029/2002JB002016.

Locardi, E., and R. Nicolich (1988), Geodinamica del tirreno e dell'appennino centro-meridionale: La nuova carta della Moho, *Mem. Soc. Geol. Ital.*, *41*, 121–140.

Lombardi, D., J. Braunmiller, E. Kissling, and D. Giardini (2008), Moho depth and poissons ratio in the western central Alps from receiver functions, *Geophys. J. Int.*, *173*, 249–264, doi:10.1111/j.1365-246X.2007.03706.x.

Maistrello, M., and G. Musacchio (2003), Archiving seismic R/WAR data from Italy and surrounding seas, *Geophys. Res. Abstr.*, *5*, 1235.

Makris, J., F. Egloff, R. Nicolich, and R. Rihma (1999), Crustal structure from the Ligurian Sea to the northern Apennines—A wide angle seismic transect, *Tectonophysics*, *301*, 305–319, doi:10.1016/S0040-1951(98)00225-X.

Malinverno, A., and W. B. F. Ryan (1986), Extension in Tyrrhenian Sea and shortening in the Apennines as result of arc migration driven by sinking of the lithosphere, *Tectonics*, *5*, 227–254, doi:10.1029/TC005i002p00227.

Marani, P., and T. Trua (2002), Thermal constriction and slab tearing at the origin of a superinflated spreading ridge: Marsilii volcano (Tyrrhenian Sea), *J. Geophys. Res.*, *107*(B9), 2188, doi:10.1029/2001JB000285.

Margheriti, L., et al. (2006), The subduction structure of the northern Apennines: Results from the RETREAT seismic deployment, *Ann. Geophys.*, *49*, 1119–1131.

Marone, F., M. van der Meijde, S. van der Lee, and D. Giardini (2003), Joint inversion of local, regional and teleseismic data for crustal thickness in the Eurasia-Africa plate boundary region, *Geophys. J. Int.*, *154*, 499–514, doi:10.1046/j.1365-246X.2003.01973.x.

Meissner, R., and W. Mooney (1998), Weakness of the lower continental crust: A condition for delamination, uplift, and escape, *Tectonophysics*, *296*, 47–60, doi:10.1016/S0040-1951(98)00136-X.

Mele, G., and E. Sandvol (2003), Deep crustal roots beneath the northern Apennines inferred from teleseismic receiver functions, *Earth Planet. Sci. Lett.*, *211*, 69–78, doi:10.1016/S0012-821X(03)00185-7.

Mele, G., E. Sandvol, and G. Cavinato (2006), Evidence of crustal thickening beneath the central Apennines (Italy) from teleseismic receiver functions, *Earth Planet. Sci. Lett.*, *249*, 425–435, doi:10.1016/j.epsl.2006.05.024.

Mooney, W., G. Laske, and T. Masters (1998), Crust 5.1: A global crustal model at 5° × 5°, *J. Geophys. Res.*, *103*, 727–747, doi:10.1029/97JB02122.

Morelli, C., S. Bellemo, I. Finetti, and G. de Visintini (1967), Preliminary depth contour maps for the Conrad and Moho discontinuities in Europe, *Bol. Geofis. Teor. Appl.*, *9*, 142–157.

Morelli, C., R. Cassinis, P. Giese, and P. Rower (1977), Structure of the lithosphere of the Italian peninsula, *Publ. Inst. Geophys. Pol. Acad. Sci.*, *115*, 451–456.

Mueller, S. (1977), A new model of the continental crust, in *The Earth's Crust: Its Nature and Physical Properties*, *Geophys. Monogr. Ser.*, vol. 20, edited by J. G. Heacock et al., pp. 289–317, AGU, Washington, D. C.

Nicholas, A., R. Polino, A. Hirn, and R. Nicholic (1991), Ecors-CROP traverse through western Alps: Results and queries, *Terra Nova Abstr.*, *3*(1), 220.

Nicolich, R., and G. Dal Piaz (1991), Isobate della Moho in Italia, in *Structural Model of Italy*, 6 fogli 1:500,000, Progetto Finalizzato "Geodinamica" CNR, Rome.

Nicolosi, I., F. Speranza, and M. Chiappini (2006), Ultrafast oceanic spreading of the Marsili Basin, southern Tyrrhenian Sea: Evidence from magnetic anomaly analysis, *Geology*, *34*, 717–720, doi:10.1130/G22555.1.

Owens, T., G. Zandt, and S. Taylor (1984), Seismic evidence for an ancient rift beneath the Cumberland Plateau, Tennessee: A detailed analysis of broadband teleseismic p waveforms, *Bull. Seismol. Soc. Am.*, *77*, 7783–7795.

Panza, G. F., A. Pontevivo, G. Chimera, R. Raykova, and A. Aoudia (2003), The lithosphere-asthenosphere: Italy and surroundings, *Episodes*, *26*(3), 169–174.

Patacca, E., and P. Scandone (2007), Geological interpretation of the CROP-04 seismic line (southern Apennines, Italy), *Bol. Soc. Geol. Ital.*, *7*, 297–315.

Pauselli, C., M. Barchi, C. Federico, B. Magnani, and G. Minelli (2006), The crustal structure of the northern Apennines (central Italy): An insight by the CROP03 seismic line, *Am. J. Sci.*, *306*(6), 428–450, doi:10.2475/06.2006.02.

Pialli, G., M. Barchi, and G. Minelli (Eds.) (1998), *Results of the Crop03 Deep Seismic Reflection Profile, Mem. Soc. Geol. Ital.*, vol. 52, 654 pp., Soc. Geol. Ital., Arezzo.

Piana Agostinetti, N., and A. Amato (2009), Moho depth and vp/vs ratio in peninsular Italy from teleseismic receiver functions, *J. Geophys. Res.*, *114*, B06303, doi:10.1029/2008JB005899.

Piana Agostinetti, N., F. P. Lucente, G. Selvaggi, and M. Di Bona (2002), Crustal structure and Moho geometry beneath the northern Apennines (Italy), *Geophys. Res. Lett.*, *29*(20), 1999, doi:10.1029/2002GL015109.

Pontevivo, A., and G. Panza (2002), Group velocity tomography and regionalization in Italy and bordering areas, *Phys. Earth Planet. Inter.*, *134*, 1–15, doi:10.1016/S0031-9201(02)00079-1.

Ponziani, F., R. De Franco, G. Minelli, G. Biella, C. Federico, and G. Pialli (1995), Crustal shortening and duplication of the Moho in the northern Apennines: A view from seismic refraction data, *Tectonophysics*, *252*, 391–418, doi:10.1016/0040-1951(95)00093-3.

Ponziani, F., R. De Franco, and G. Biella (1998), Geophysical reinterpretation of 1974 and 1978 DSS experiments along CROP profile, *Mem. Soc. Geol. Ital.*, *52*, 193–203.

Roselli, P., F. P. Lucente, and N. Piana Agostinetti (2008), Crustal structure at the Tyrrhenian-Adriatic domain boundary from receiver functions analysis in northern Apennines (Italy), *Geophys. Res. Lett.*, *35*, L12304, doi:10.1029/2008GL034055.

Royden, L. (1988), Flexural behavior of the continental lithosphere in Italy: Constraints imposed by gravity and deflection data, *J. Geophys. Res.*, *93*, 7747–7766, doi:10.1029/JB093iB07p07747.

Sartori, R., et al. (1989), Drillings of ODP leg 107 in the Tyrrhenian Sea: Tentative basin evolution compared to deformations in the surrounding chains, in *The Lithosphere in Italy*, edited by A. Boriani et al., pp. 139–156, Acad. Naz. dei Lincei, Rome.

Sartori, R., G. Carrara, L. Torelli, and N. Zitellini (2001), Neogene evolution of the southwestern Tyrrhenian Sea (Sardinia basin and western bathyal plain), *Mar. Geol.*, *175*, 47–66, doi:10.1016/S0025-3227(01)00116-5.

Sartori, R., L. Torelli, N. Zitellini, G. Carrara, M. Magaldi, and P. Mussoni (2004), Crustal features along a W-E Tyrrhenian transect from Sardinia to Campania margins (central Mediterranean), *Tectonophysics*, *383*, 171–192, doi:10.1016/j.tecto.2004.02.008.

Scarascia, S., A. Lozej, and R. Cassinis (1994), Crustal structures of the Ligurian, Tyrrhenian and Ionian seas and adjacent onshore areas interpreted from wide-angle seismic profiles, *Bol. Geofis. Teor. Appl.*, *36*, 5–19.

Schmid, S., B. Fügenschuh, E. Kissling, and R. Schuster (2004), Tectonic map and overall architecture of the Alpine orogen, *Eclogae Geol. Helv.*, *97*, 93–117, doi:10.1007/s00015-004-1113-x.

Scrocca, D., et al. (Eds.) (2003), *CROP ATLAS: Seismic Reflection Profiles of the Italian Crust, Mem. Desc. Carta Geol. Ital.*, vol. 62, 193 pp., Ist. Poligrafico e Zecca dello Stato, Roma.

Solarino, S., D. Spallarossa, S. Parolai, M. Cattaneo, and C. Eva (1996), Lithoasthenospheric structures of northern Italy as inferred from teleseismic P wave tomography, *Tectonophysics*, *260*, 271–289, doi:10.1016/0040-1951(95)00201-4.

Solarino, S., E. Kissling, S. Sellami, G. Smiriglio, F. Thouvenot, M. Granet, K. Bonjer, and D. Sleijko (1997), Compilation of a recent seismicity data base of the greater Alpine region from several seismological networks and preliminary 3D tomographic results, *Ann. Geophys.*, *40*, 161–214.

Speranza, F., and M. Chiappini (2002), Thick-skinned tectonics in the external Apennines, Italy: New evidence from magnetic anomaly analysis, *J. Geophys. Res.*, *107*(B11), 2290, doi:10.1029/2000JB000027.

Stampfli, G., and G. Borel (2002), A plate tectonic model for the Paleozoic and Mesozoic constrained by dynamic plate boundaries and restored synthetic oceanic isochrones, *Earth Planet. Sci. Lett.*, *196*, 17–33, doi:10.1016/S0012-821X(01)00588-X.

Steckler, M., N. Piana Agostinetti, C. Wilson, P. Roselli, L. Seeber, A. Amato, and A. Lerner-Lam (2008), Crustal structure in the southern Apennines from teleseismic receiver functions, *Geology*, *36*, 155–158, doi:10.1130/G24065A.1.

Steinmetz, L., F. Ferrucci, A. Hirn, C. Morelli, and R. Nicolich (1983), A 550 km long Moho traverse in the Tyrrhenian Sea from OBS recorded Pn phases, *Geophys. Res. Lett.*, *10*, 428–431, doi:10.1029/GL010i006p00428.

Suhadolc, P., and G. Panza (1989), Physical properties of the lithosphere-asthenosphere system in Europe from geophysical data, in *The Lithosphere in Italy*, edited by A. Boriani et al., pp. 15–40, Acad. Naz. dei Lincei, Rome.

Tesauro, M., M. Kaban, and S. Cloetingh (2008), EuCRUST-07: A new reference model for the European crust, *Geophys. Res. Lett.*, *35*, L05313, doi:10.1029/2007GL032244.

TRANSALP Working Group (2002), First deep seismic reflection images of the eastern Alps reveal giant crustal wedges and transcrustal ramps, *Geophys. Res. Lett.*, *29*(10), 1452, doi:10.1029/2002GL014911.

van der Meijde, M., S. van der Lee, and D. Giardini (2003), Crustal structure beneath broad-band seismic stations in the Mediterranean region, *Geophys. J. Int.*, *152*, 729–739, doi:10.1046/j.1365-246X.2003.01871.x.

Ventura, G., G. Vilardo, G. Milano, and N. Pino (1999), Relationships among crustal structure, volcanism and strike-slip tectonics in the Lipari-Vulcano volcanic complex (Aeolian Islands, southern Tyrrhenian Sea, Italy), *Phys. Earth Planet. Inter.*, *116*, 31–52, doi:10.1016/S0031-9201(99)00117-X.

Waldhauser, F. (1996), A parameterized three-dimensional Alpine crustal model and its application to teleseismic wavefront scattering, Ph.D. thesis, Swiss Fed. Inst. of Technol., Zurich, Switzerland.

Waldhauser, F., E. Kissling, J. Ansorge, and S. Muller (1998), Three-dimensional interface modeling with two-dimensional seismic data: The Alpine crust-mantle boundary, *Geophys. J. Int.*, *135*, 264–278, doi:10.1046/j.1365-246X.1998.00647.x.

Waldhauser, F., R. Lippitsch, E. Kissling, and J. Ansorge (2002), High-resolution teleseismic tomography of upper-mantle structure using an a priori three-dimensional crustal model, *Geophys. J. Int.*, *150*, 403–414, doi:10.1046/j.1365-246X.2002.01690.x.

Ye, S., J. Ansorge, E. Kissling, and S. Mueller (1995), Crustal structure beneath the eastern Swiss Alps derived from seismic refraction data, *Tectonophysics*, *242*, 199–221, doi:10.1016/0040-1951(94)00209-R.

Zhu, L., and H. Kanamori (2000), Moho depth variation in Southern California from teleseismic receiver functions, *J. Geophys. Res.*, *105*, 2969–2980.